Journal of Current Science and Technology, April-June 2026 Vol. 16 No. 2, Article 169

ISSN 2630-0656 (Online)

Cite this article: Emudom, V., & Singhasani, M. (2026). Effect of magnetic field on heat transfer enhancement and pressure drop of fluid flow with magnetic particle suspension in a curled pipe. *Journal of Current Science and Technology*, *16*(2), Article 169. https://doi.org/10.59796/jcst.V16N2.2026.169

Journal of Current Science and Technology

Journal homepage: https://jcst.rsu.ac.th

Effect of Magnetic Field on Heat Transfer Enhancement and Pressure Drop of Fluid Flow with Magnetic Particle Suspension in a Curled Pipe

Varut Emudom*, and Monta Singhasani

Department of Mechanical Engineering, College of Engineering, Rangsit University, Pathum Thani 12000, Thailand

*Corresponding author; E-mail: varutama8008@gmail.com

Received 25 August 2025; Revised 11 September 2025; Accepted 6 October 2025; Published online 25 March 2026

Abstract

The characteristics of heat transfer enhancement and pressure drop in the curled pipe under the effect of a magnetic field are presented in this paper. The suspensions, which are composed of γ-Fe_2O_3 (gamma-phase iron oxide) magnetic particles with a median diameter of 15–20 nm dispersed in plain water have been used. The magnetic particles at different concentrations by volume of 0.50%, 0.75% and 1.00% were used in the pipe flow experiments. The suspension enters the curled pipe at the innermost turn, flows under a uniform surface heat flux, and exits at the outermost turn. To increase the rate of heat transfer, three different strengths of an external magnetic field of 600 Gauss (G), 1,200 G, and 1,800 G were utilized by the electromagnets mounted on plates located at the top and bottom of the curled pipe. The effects of magnetic field strength, concentration by volume of magnetic particles, and curve ratios on the heat transfer enhancement and pressure drop are shown. The results show that the Nusselt number increases with increasing magnetic field strength, particle volume concentration, and curve ratio. The Nusselt number increased by up to 14.34%, 19.19%, and 26.26% for magnetic field strengths of 600 G, 1,200 G, and 1,800 G, respectively.

Keywords: *heat transfer enhancement; pressure drop; magnetic field; gamma-type iron oxides; surface heat flux; curve ratio*

1. Introduction

The efficiency of many engineering equipment can be improved with limitations by using conventional heat transfer fluids such as water and oil which have low thermal conductivity. Heat transfer fluids with high thermal conductivity can be used to improve the efficiency of many engineering apparatus which relate to the heat transfer including the electronic devices and heat exchangers. To keep electronic devices operating within the design temperature range, the performance of their thermal cooling is a critical issue. One innovative approach is the use of very small magnetic particles as a discontinuous medium to increase the thermal conductivity of the fluids. To be uniformly suspended in a liquid, the median size of magnetic particles should be less than 25 nm. A crucial parameter affecting energy transport in magnetic particle suspensions is the solid volume concentration. Many experiments show remarkable improvements in effective thermal conductivity (Esfe et al., 2019; Jeong et al., 2013). By increasing the magnetic field strength, the ratio of the thermal conductivity of magnetic particle suspensions to that of plain water can be increased (Karimi et al., 2015). Another study reports that the thermal conductivity of magnetic particle suspensions can increase rapidly with the volume concentration of particles (Hojjat et al., 2011). The heat transfer properties of a fuel oil nanofluid were investigated for flow inside vertical curled tubes at different concentrations (Pakdaman et al., 2012). Using the spectral method for numerical studies, the investigators studied the effect of incompressible fluid flow in a helically coiled pipe (Hoque & Alamb, 2013). The mass and temperature distributions of

nanofluids flowing peristaltically were studied numerically in a curved channel under the influence of a magnetic field (Noreen et al., 2015). The temperature and velocity distributions of fluid in a curled channel subjected to a magnetic field were studied (Hayat et al., 2016). To keep the magnetic particles thoroughly dispersed in the fluid, the magnetic particles are coated with layers of surfactants and are typically very small, with diameters ranging from 10 nm to 30 nm (Liou et al., 2019). Some magnetic particles may agglomerate caused by the dipole-dipole interactions (Khodadadi et al., 2019). The suspensions do not maintain any net magnetization, and the magnetic particles are randomly oriented when no external magnetic field is applied. However, when an external magnetic field is imposed on suspensions, the magnetic particles tend to align, forming chain-like structures (Arabpour et al., 2018). Because the magnitude of the external magnetic field and the temperature variation can be manually controlled and imposed on magnetic particle suspensions, these suspensions can play a crucial role in several heat transfer applications. For applications in heating and cooling systems, other researchers investigated the viscosity of magnetic particle suspensions (Bahiraei & Hangi, 2015). The effects of the frequency of the oscillating applied magnetic field were investigated to determine variations in local heat transfer coefficients (Yarahmadi et al., 2015). Another study examined the use of Fe_3O_4 magnetic particles in a helically coiled tube heat exchanger both numerically and experimentally (Ghaderi et al., 2022). The study found that, as the coil inlet temperature increased, the overall Nusselt number increased by 22%. An article presented a combination of experimental and numerical methods to show that the efficiency of shell and helically coiled heat exchangers could be improved by 7.68% using Al_2O_3 nanoparticles (Abdullah & Hussein, 2023). The ferromagnetic nanofluid was investigated numerically using a two-phase model for flow inside a heat exchanger equipped with helical ribs (Varkaneh et al., 2023). A mixture of water and aluminum oxide nanoparticles was used to enhance the heat transfer rate in the shell-and-helical-coil tube heat exchanger with a wider range of particle concentrations varying from 0.0% to 0.75% (Shabi et al., 2024). The results suggest that the nanoparticles significantly improve the heat transfer coefficient inside the helically coiled tube. Many previous studies presented heat transfer enhancement in the curled pipe with and without the effect of a magnetic field by carrying out experiments based solely on constant surface temperature, both experimentally and numerically.

In this study, heat transfer performance was examined by conducting all experiments on the basis of constant surface heat flux. Magnetic particle suspensions were utilized to investigate heat transfer performance in the horizontal curled pipe. The crucial aspects, namely the magnetic field strength, the volume concentrations of magnetic particles, and the curve ratios, were the primary goals, which are beneficial for identifying reasonable alternatives for heat transfer enhancement.

2. Objectives

The principal purposes of this study are to demonstrate several crucial aspects, namely the volume concentrations of magnetic particles in the suspensions, the strengths of the applied magnetic field and the curve ratio, which have crucial effects on heat transfer performance and pressure drop in curled pipe flow. The enhancement in heat transfer can be maximized by increasing the volume concentrations of magnetic particles in the suspensions, the strengths of the applied magnetic field and the curve ratio.

3. Materials and Methods

3.1 Apparatus

A schematic diagram of the experimental apparatus is shown in Figure 1 for flow experiments in the horizontal curled pipe.

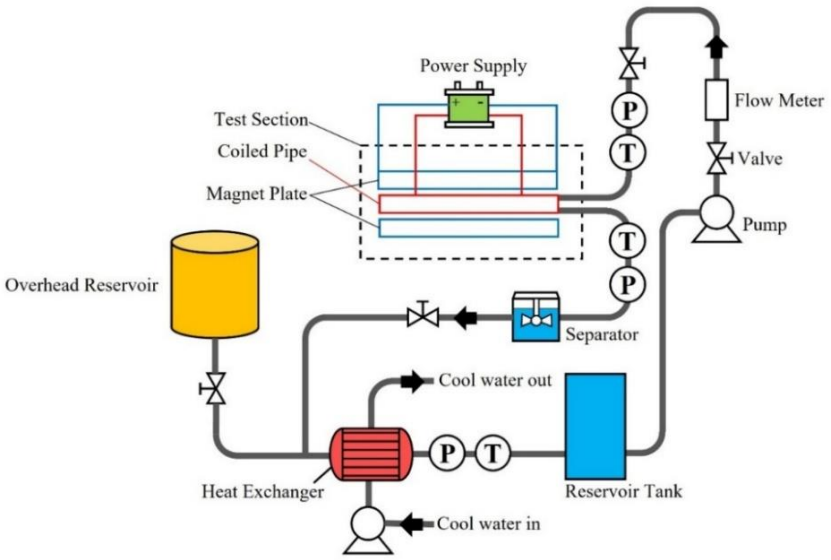

Figure 1 Schematic diagram of the experimental apparatus

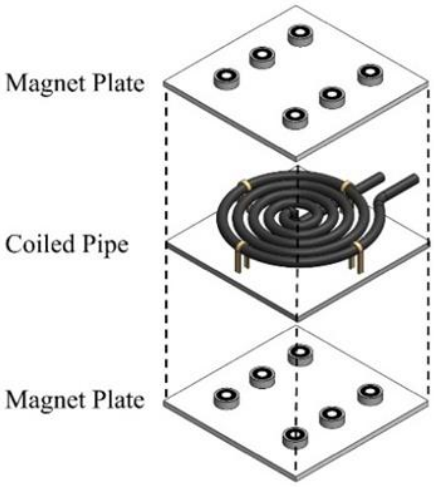

Figure 2 Schematic diagram of the test section

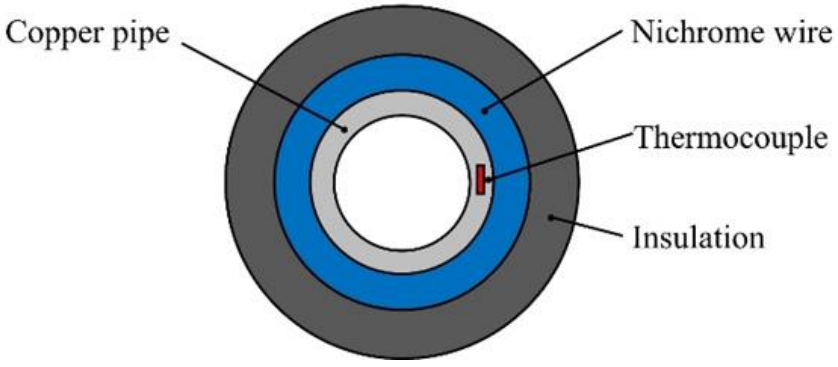

Figure 3 Cross section of the test pipe

Table 1 Dimensions of the curled pipe

Parameters	Dimensions
Internal and external diameters, mm	9.5, 10.5
Length of test pipe, mm	115, 150, 240
Curve ratio, (D_p / D_c)	0.05, 0.03, 0.015
Number of coiled turns	5
Spacing of curled pipe, mm	15, 22, 45

The experimental system consists of a heated test section, a flow loop, electromagnets, a heat exchanger, and measuring and controlling units. The test section consists of a horizontal curled copper pipe with 9.5 mm internal diameter and 10.5 mm external diameter. All dimensions of the curled pipe are given in Table 1.

Six electromagnets were mounted on a thin plastic plate placing on top of the curled pipe, and six electromagnets were mounted on another thin plastic plate placed at the bottom of the curled pipe as shown in Figure 2. The magnetic plates were measured to be 680 mm x 680 mm.

Heating was achieved by applying a uniform surface heat flux to the copper pipe by encasing Nichrome wire along the pipe. A power supply with a maximum power of 600 W was connected to the Nichrome wire to generate sufficient heat at the surface of the copper pipe. To prevent heat transfer loss, the copper pipe was wrapped with rubber and aluminium foil as insulation. Figure 3 shows the cross-section of the test pipe. The heat exchanger was used to maintain a stable temperature of the magnetic particle suspensions at the entrance of the test section. Ten thermocouples were used to measure the temperature distribution of the magnetic particle suspensions along the curled pipe. All thermocouples were initially calibrated using a dry-block calibrator with a precision of 0.01 ºC. The pressure transducer was employed to measure the static pressure drop by measuring the pressure difference between the inlet and outlet of the curled pipe. The pressure transducer was initially calibrated using a deadweight tester to ensure an accuracy of ± 0.01%.

3.2 Materials

A combination of magnetic particles with a median size of 20 nm and plain water was utilized as the magnetic particle suspensions in this study. The gamma-type iron oxide is recognized for their cubic structures and the individual atoms' moments are aligned in the same direction (Rosensweig, 1997). The majority of the magnetic particles dispersed in plain water were nearly circular in shape and in the form of large clusters. Before conducting the experiments, the magnetic particles were ultrasonicated for 30 minutes to break up any clusters or agglomerates. The magnetic particles were then allowed to rest at room temperature for 2 hours after ultrasonication to reduce any heating effects. Without using any surfactant, the magnetic particle suspensions with three different volume concentrations (0.50%, 0.75%, and 1.00%) were then prepared by stirring continuously in an ultrasonic bath system for an hour until stable suspensions were achieved.

3.3 Mathematical Model

The total rate of heat transfer absorbed by the magnetic particle suspensions flowing through the entire curled pipe can be computed using the following equation:

$$Q_{conv} = \mathrm{m}\, C_{p,mps}\, (T_{m,out} - T_{m,in}) \quad (1)$$

where Q_{conv} is the total rate of heat transfer, $T_{m,out}$ and $T_{m,in}$ are the median values of the exit and entrance temperatures of the magnetic particle suspensions, m is the mass flow rate of the suspensions and $C_{p,mps}$ is the specific heat of the magnetic particle suspensions.

The average heat transfer rate can be computed using the following equation:

$$Q_{ave} = [\mathrm{IV} + \mathrm{m}\, C_{p,mps}\, (T_{m,out} - T_{m,in})] / 2 \quad (2)$$

where Q_{ave} is the average heat transfer rate, I is the current and V is the supplied voltage.

The specific heat of the magnetic particle suspensions is proposed as follows (Xuan & Roetzel, 2000):

$$\rho_{mps}\, C_{p,mps} = (1 - \phi)(\rho_w\, C_{p,w}) + \phi\, (\rho_{mp}\, C_{p,mp}) \quad (3)$$

where $C_{p,mps}$ is the specific heat of the magnetic particle suspensions, ρ_{mps} is the density of the magnetic particle suspensions, ϕ is the concentration by volume of magnetic particles in the suspensions, ρ_w is the density of water, $C_{p,w}$ is the specific heat of water, ρ_{mp} is the density of the magnetic particles and $C_{p,mp}$ is the specific heat of the magnetic particles.

The density of the magnetic particle suspensions is determined by the correlation proposed as follows (Pak & Cho, 1998):

$$\rho_{mps} = (1 - \phi)\, \rho_w + \phi\, \rho_{mp} \quad (4)$$

The heat transfer coefficient of the magnetic particle suspensions can be determined from the following equation:

$$h = (Q_{conv} / A_s) / (T_s - T_m) \quad (5)$$

where h is the heat transfer coefficient, Q_{conv} / A_s is the constant surface heat flux, A_s is the heat transfer surface area of the curled pipe, T_s is the surface temperature of the tested pipe and T_m is the median temperature of the magnetic particle suspensions.

The Nusselt number (Nu) in heat transfer is a dimensionless number that indicates the ratio of heat transfer by convection to heat transfer by conduction. It essentially identifies how effectively heat is transferred by convection compared with conduction in stagnant fluid. It can be calculated using the following equation:

$$Nu = h D / k_{mps} \quad (6)$$

where Nu is the Nusselt number, D is the pipe internal diameter and k_{mps} is the thermal conductivity of the magnetic particle suspensions.

The predicted value of the thermal conductivity of the magnetic particle suspensions is suggested as follows (Drew & Passman, 1999):

$$k_{mps} = k_w \times [(k_{mp} + 2k_w - 2\phi (k_w - k_{mp}) / (k_{mp} + 2k_w + \phi (k_w - k_{mp})] \quad (7)$$

where k_w is the thermal conductivity of water and k_{mp} is the thermal conductivity of magnetic particles.

The Reynolds number of the magnetic particle suspensions is calculated based on the internal diameter of the pipe as follows:

$$Re_D = (\rho_{mps} U_{mps} D) / \mu_{mps} \quad (8)$$

where Re_D is the Reynolds number, U_{mps} is the velocity of the magnetic particle suspensions, and μ_{mps} is the predicting viscosity of the magnetic particle suspensions.

The predicted viscosity of the magnetic particle suspensions is determined by the correlation proposed as follows (Drew & Passman, 1999):

$$\mu_{mps} = \mu_w (1 + 2.5 \phi) \quad (9)$$

where μ_{mps} is the viscosity of the magnetic particle suspensions and μ_w is the viscosity of the water.

The Dean number (De) is a dimensionless number used to characterize fluid flow inside a curled pipe. It combines the effects of centrifugal and inertial forces. The dean number can be computed as follows:

$$De = Re_D \times (D / R_c)^{0.5} \quad (10)$$

where De is the Dean number and R_c is the curvature radius.

The friction factor (f) is a dimensionless number that indicates the pressure drop occurring inside the curled pipe. The pressure drop is the energy loss caused by friction between the magnetic particle suspensions and the pipe wall. The friction factor can be computed as follows:

$$f = (\Delta P/L \times D) / (0.5 \rho_{mps} V^2) \quad (11)$$

where f is the friction factor, $\Delta P/L$ is the pressure drop per unit pipe length, ρ_{mps} is the density of the magnetic particle suspensions and V is the velocity of the suspensions.

3.4 Uncertainty Evaluation

The uncertainty (σ) can arise from inaccuracies in the measured data. The applied heat flux, the surface temperature of the copper tube, the supplied voltage, and the measured electric current are among the data causing inaccuracies. The uncertainty of the heat transfer coefficient can be computed as follows:

$$\sigma_h = \pm \sqrt{\left(\frac{\partial h}{\partial q_s''}\sigma_{q_s''}\right)^2 + \left(\frac{\partial h}{\partial T_s}\sigma_{T_s}\right)^2 + \left(\frac{\partial h}{\partial T_m}\sigma_{T_m}\right)^2} \quad (12)$$

The uncertainty of the median temperature of the suspension can be computed as follows:

$$\sigma_{T_m} = \pm \sqrt{\left(\frac{\partial T_m}{\partial T_{m,i}}\sigma_{T_{m,i}}\right)^2 + \left(\frac{\partial T_m}{\partial y}\sigma_y\right)^2} \quad (13)$$

For all cases, the uncertainty parameters were computed. The average uncertainty of the heat transfer coefficients was calculated to be ± 0.38%. The average uncertainty of the median temperature of the suspension was calculated to be ± 0.10 °C.

4. Results

In the experiments, the magnetic particle suspensions flowed along the curled pipe by entering the innermost turn and flowing out at the outermost turn to absorb heat from the applied surface heat flux. The curled pipe is located between two parallel plates that comprise the installed electromagnets. The magnetic fields created by the two magnetic plates are perpendicular to the suspensions' flow inside the curled pipe. To verify the experimental equipment and procedures, our data were initially compared with other correlations. Figure 4 shows a comparison of the obtained Nusselt number at magnetic field strengths of 1,200 G and 1,800 G with the Nusselt number from the correlations proposed by Wu et al. (2013) and Xin et al. (1997). The proposed correlations were developed for fluid flow inside the curled pipe without the effect of a magnetic field. The trend in our obtained Nusselt numbers of fluid flow inside the curled pipe under the effect of a magnetic field considerably concurs with the predicted results of the mentioned correlations. Our results are higher than those predicted by the correlations because of the magnetic field effect.

Figures 5-7 show the effect of the magnetic field on the median temperature of the suspension at different volume concentrations. The curve ratio is 0.015.

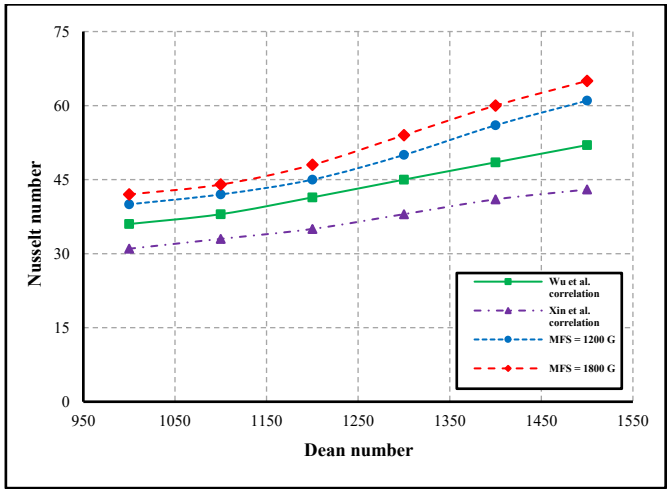

Figure 4 Comparison between obtained Nusselt number from this experiment and results from other correlations for the curled pipe.

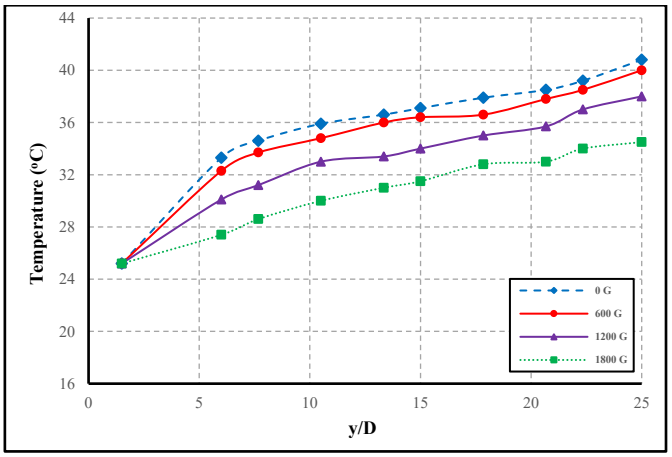

Figure 5 Effect of magnetic field on the median temperature of the suspension at concentration by volume of 0.50%.

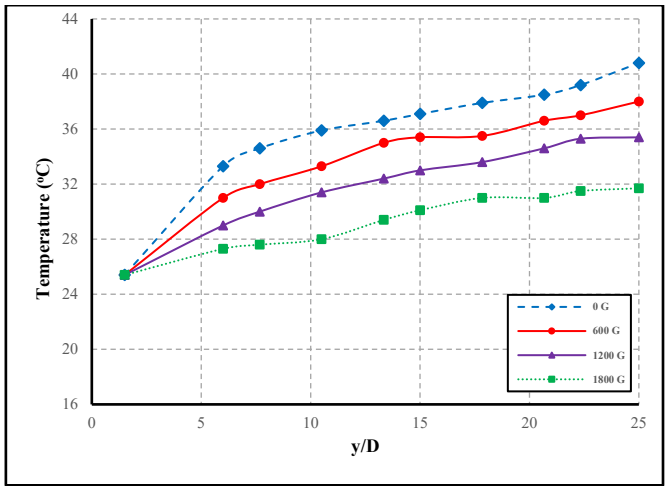

Figure 6 Effect of magnetic field on the median temperature of the suspension at concentration by volume of 0.75%.

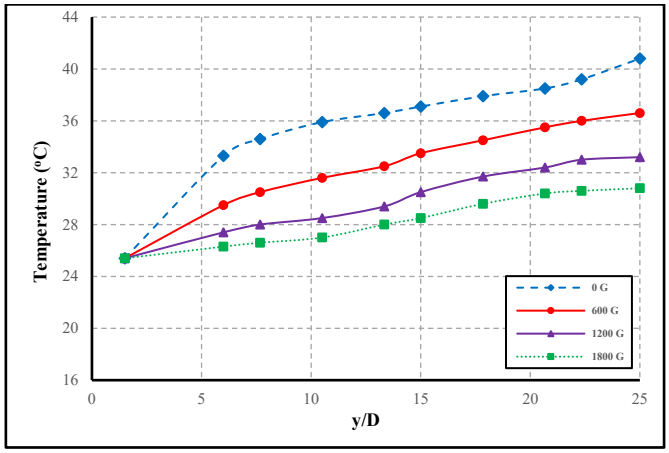

Figure 7 Effect of magnetic field on the median temperature of the suspension at concentration by volume of 1.00%.

From Figures 5-7, as the concentration increases, the median temperature of the magnetic particle suspensions tends to decrease markedly at higher magnetic field strengths. Compared with the case with no application of the magnetic field, a temperature decrease of 10.0 °C was observed at a magnetic field strength of 1,800 G and a volume concentration of 1.00%. Figures 8-10 show the variations in the Nusselt number and the Reynolds number of the magnetic particle suspensions for different curve ratios at different strengths of the applied magnetic field. The volume concentration of the magnetic particles is 0.75%.

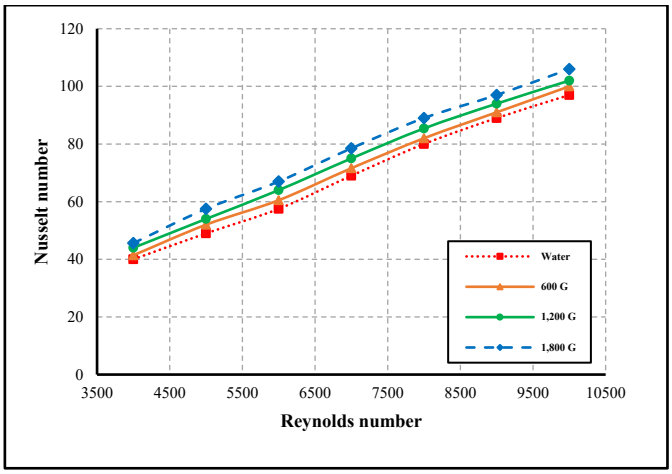

Figure 8 Effect of different strengths of the magnetic field on the Nusselt number for the curve ratio of 0.015.

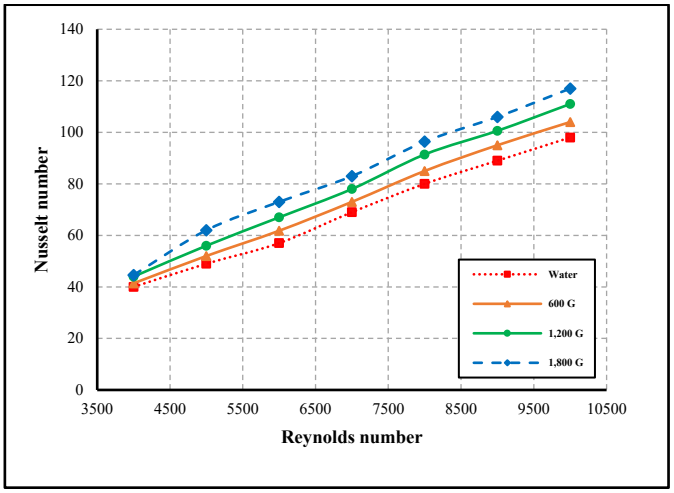

Figure 9 Effect of different strengths of the magnetic field on the Nusselt number for the curve ratio of 0.03.

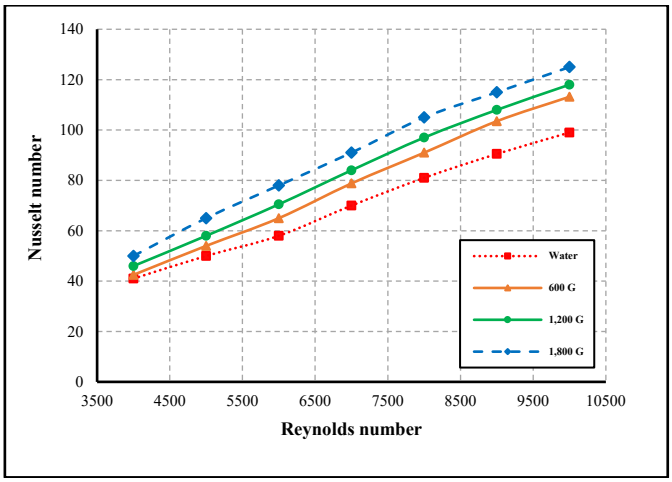

Figure 10 Effect of different strengths of the magnetic field on the Nusselt number for the curve ratio of 0.05.

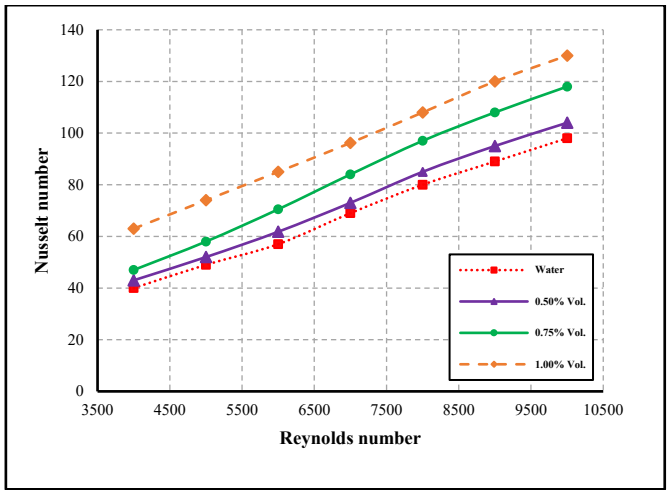

Figure 11 Effect of the different concentration by volume on the Nusselt number for the curve ratio of 0.05.

From Figures 8–10, increasing the Reynolds number enhances heat transfer capability. The Nusselt number increases with increasing flow rate of the suspension. The magnetic particle suspensions have a better heat transfer capability than plain water because of the suspended magnetic particles. From these figures, the flow of magnetic particle suspensions through the curled pipe can provide a Nusselt number higher than that of plain water. The centrifugal and magnetic forces play a crucial role in accelerating the magnetic particle suspensions as they flow along the curled pipe under the applied magnetic field. Increasing the curve ratio by making the coil tighter can also enhance heat transfer. As the suspensions flow through a curved pipe, centrifugal forces push the faster-moving parts of the suspensions in the pipe core towards the outer wall. Continuity of the flow is maintained as the slower-moving parts of the suspensions near the pipe wall are pushed towards the inner wall. A swirling motion is then created perpendicular to the main flow. The attraction and breakup of the magnetic particles in the suspensions caused by the swirling motion can have an essential effect to create higher disturbance in the thermal boundary zone. Thus, the magnetic particle suspensions under high magnetic field strengths can provide a higher Nusselt number. Figure 11 shows the effects of the volume concentration of the magnetic particles in the suspensions on the Nusselt number. The curve ratio is 0.05 and the strength of the magnetic field is 1,200 G.

From Figure 11, the heat transfer mechanism involves an increased accumulation of magnetic particles near the heated pipe wall as the volume concentration of magnetic particles in the suspensions increases. The accumulation of magnetic particles can disturb the thermal boundary layer, creating substantial turbulence and a high enhancement in heat transfer. Figures 12-14 show the effect of different strengths of the magnetic field on the friction factor for the curve ratio of 0.015, 0.03 and 0.05, respectively. The volume concentration of magnetic particles is 1.00%. From these figures, the friction factor tends to increase with the increasing flow rate of the magnetic particle suspensions. With a higher curve ratio, resulting from a lower average curvature radius, the centrifugal force in the secondary flow causes the pressure drop to increase much more than in flow with a lower curve ratio. Also, the pressure drop is likely to increase in suspension flow under higher magnetic field strengths.

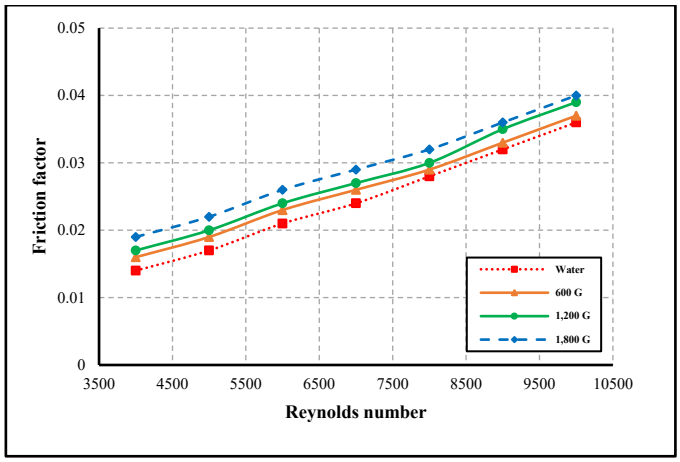

Figure 12 Effect of different strengths of the magnetic field on friction factor for the curve ratio of 0.015.

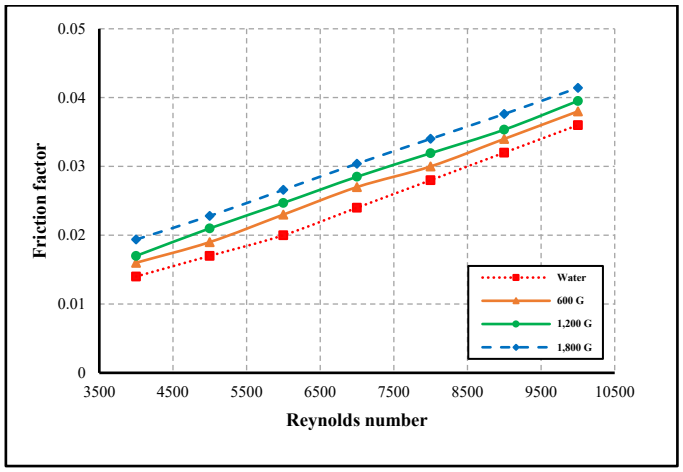

Figure 13 Effect of different strengths of the magnetic field on friction factor for the curve ratio of 0.03.

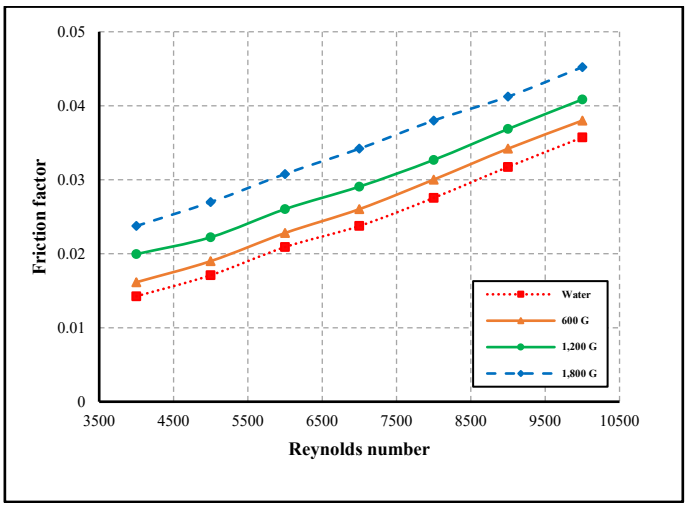

Figure 14 Effect of different strengths of the magnetic field on friction factor for the curve ratio of 0.05.

From Figures 12-14, the friction factor tends to increase with the increasing flow rate of the magnetic particle suspensions. With a higher curve ratio, resulting from a lower average curvature radius, the centrifugal force in the secondary flow causes the pressure drop to increase much more than in flow with a lower curve ratio. Also, the pressure drop tends to increase in suspension flow under higher magnetic field strengths.

5. Discussion

The proposed parameters, namely the magnetic field strength, the volume concentration of magnetic particles in the suspensions, and the curve ratio, affect heat transfer enhancement in curled pipe flow. Higher values of magnetic field strength, volume concentration, and curve ratio enhances heat transfer performance. Making the coil radius tighter, thereby increasing the curve ratio, can play a crucial role in enhancing heat transfer. Centrifugal forces significantly enhance the mixing of the suspensions. This can disturb the thermal boundary layer and reduce any thermal resistance, leading to a higher heat transfer coefficient and Nusselt number. Increasing the volume concentration of magnetic particles in the suspensions can improve convective heat transfer. The magnetic moments inside the magnetic particles are usually positioned irregularly when no magnetic field is applied. Brownian motion mainly affects the magnetic particles because thermal energy is higher than the energy of the magnetic dipoles (Rosensweig, 1997). Mostly, very small particles suspended in a carrier liquid are in arbitrary motion caused by Brownian motion. The energy of magnetic dipoles grows more powerful and can subdue Brownian thermal energy when the magnetic particle suspensions are subjected to an external magnetic field. The orientation of magnetic particles is caused by the adjustment of magnetic moments to line up in the direction of the magnetic field, creating clusters and several small train-like structures. The strength of magnetic field increases the formation of these magnetic particles in train-like structures. When the volume concentration of the magnetic particles increases, the train-like structures become linear and elongate. Heat transfer can perform remarkably well under this condition. Increasing the thermal conductivity of the magnetic particle suspensions can also enhance forced convection heat transfer. Magnetic torque in the magnetic particles is the main mechanism governing the thermal conductivity of the magnetic particle suspensions (Keyvani et al., 2018). Magnetic torque helps to align the magnetic particles' magnetic moments in the same direction as the applied magnetic field. The thermal conductivity of the magnetic particle suspensions can be increased by increasing the strength of the magnetic field. Thus, the heat transfer enhancement can be achieved reasonably well. The main disadvantage of increasing the curve ratio, the volume concentration of magnetic particles in the suspensions, and the strength of the applied magnetic field is an increase in pressure drop and friction factor along the curled pipe. However, the increase in pressure drop was relatively minor compared with the enhancement in heat transfer. Future work could be conducted by utilizing an oscillating magnetic field, comparing pulsating and continuous flow, using hybrid oxides in the suspension, or validating the experimental data with CFD simulations.

6. Conclusion

The heat transfer performance of suspensions consisting of Fe_2O_3 magnetic particles was investigated experimentally in a curled pipe. By applying a magnetic field to the magnetic particle suspensions, heat transfer performance was improved. The results revealed that the heat transfer coefficient, and hence the Nusselt number, increased with increasing volume concentration of magnetic particles, applied magnetic field strength, and curve ratio. Centrifugal forces in the secondary flows had a significant effect on the mixing of magnetic particles in plain water. Heat transfer performance can be attained satisfactorily by using a volume concentration of 1.00%, a magnetic field strength of 1,800 G, and a curve ratio of 0.05. However, However, these improvements are accompanied by an increase in pressure drop in the curled pipe.

7. Abbreviations

Abbreviation	Full Term
A_s	Heat transfer surface area
$C_{p,mp}$	Specific heat of magnetic particles
$C_{p,mps}$	Specific heat of magnetic particle suspension
$C_{p,w}$	Specific heat of water
D	Pipe internal diameter
De	Dean number
f	Friction factor
G	Unit of magnetic field strength
h	Heat transfer coefficient
I	Electric current

Abbreviation	Full Term
k_{mp}	Thermal conductivity of magnetic particles
k_{mps}	Thermal conductivity of magnetic particle suspension
k_w	Thermal conductivity of water
m	Mass flowrate
Nu	Nusselt number
ΔP/L	Pressure drop per unit pipe length
Q_{ave}	Average heat transfer rate
Re_D	Reynolds number
R_c	Curvature radius
T_m	Median temperature of magnetic particle suspension
T_s	Surface temperature of the tested pipe
U_{mps}	Velocity of magnetic particle suspension
V	Supplied voltage
ρ_{mp}	Density of magnetic particles
ρ_{mps}	Density of magnetic particle suspension
ρ_w	Density of water
μ_{mps}	Viscosity of magnetic particle suspension
μ_w	Viscosity of water
ϕ	Concentration by volume of magnetic particles in the suspension
σ_h	Uncertainty of heat transfer coefficient
$\sigma_{q"s}$	Uncertainty of surface heat flux
σ_{Tm}	Uncertainty of median temperature
σ_{Ts}	Uncertainty of surface temperature
σ_y	Uncertainty of axial distance

8. Acknowledgements

The authors would like to thank the Department of Mechanical Engineering and Rangsit University for their support.

9. CRediT Statement

Varut Emudom: Conceptualization, Methodology, Software, Validation, Formal Analysis, Investigation, Resources, Data Curation, Writing-Original Draft, Writing-Review & Editing, Visualization, Supervision, and Project Administration.

Monta Singhasani: Drawing schematic diagram of the experimental apparatus and schematic diagram of the test section.

10. References

Abdullah, M. S., & Hussein, A. M. (2023). Experimental and numerical investigations on the heat transfer of a helical coil heat exchanger utilized α-Al_2O_3 nanofluid. *Diyala Journal of Engineering Sciences*, *16*(3), 64–81. https://doi.org/10.24237/djes.2023.16306

Arabpour, A., Karimipour, A., & Toghraie, D. (2018). The study of heat transfer and laminar flow of kerosene/multi-walled carbon nanotubes (MWCNTs) nanofluid in the microchannel heat sink with slip boundary condition. *Journal of Thermal Analysis and Calorimetry*, *131*(2), 1553-1566. https://doi.org/10.1007/s10973-017-6649-x

Bahiraei, M., & Hangi, M. (2015). Flow and heat transfer characteristics of magnetic nanofluids: A review. *Journal of Magnetism and Magnetic Materials*, *374*, 125-138. https://doi.org/10.1016/j.jmmm.2014.08.004

Drew, D. A., & Passman, S. L. (1999). *Theory of multicomponent fluids*. Springer Science & Business Media.

Esfe, M. H., Raki, H. R., Emami, M. R. S., & Afrand, M. (2019). Viscosity and rheological properties of antifreeze based nanofluid containing hybrid nano-powders of MWCNTs and TiO_2 under different temperature conditions. *Powder Technology*, *342*, 808-816. https://doi.org/10.1016/j.powtec.2018.10.032

Ghaderi, A., Veysi, F., Aminian, S., Andami, Z., & Najafi, M. (2022). Experimental and numerical study of thermal efficiency of helically coiled tube heat exchanger using ethylene glycol-distilled water based Fe_3O_4 nanofluid. *International Journal of Thermophysics*, *43*(8), Article 118. https://doi.org/10.1007/s10765-022-03041-w

Hayat, T., Tanveer, A., Alsaadi, F., & Mousa, G. (2016). Impact of radial magnetic field on peristalsis in curved channel with convective boundary conditions. *Journal of Magnetism and Magnetic Materials*, *403*, 47-59. https://doi.org/10.1016/j.jmmm.2015.11.078

Hojjat, M., Etemad, S. G., Bagheri, R., & Thibault, J. (2011). Thermal conductivity of non-Newtonian nanofluids: Experimental data and modeling using neural network. *International Journal of Heat and Mass Transfer*, *54*(5-6), 1017-1023. https://doi.org/10.1016/j.ijheatmasstransfer.2010.11.039

Hoque, M. M., & Alam, M. M. (2013). Effects of Dean number and curvature on fluid flow through a curved pipe with magnetic field.

Procedia Engineering, *56*, 245-253. https://doi.org/10.1016/j.proeng.2013.03.114

Jeong, J., Li, C., Kwon, Y., Lee, J., Kim, S. H., & Yun, R. (2013). Particle shape effect on the viscosity and thermal conductivity of ZnO nanofluids. *International Journal of Refrigeration*, *36*(8), 2233-2241. https://doi.org/10.1016/j.ijrefrig.2013.07.024

Karimi, A., Goharkhah, M., Ashjaee, M., & Shafii, M. B. (2015). Thermal conductivity of Fe_2O_3 and Fe_3O_4 magnetic nanofluids under the influence of magnetic field. *International Journal of Thermophysics*, *36*(10), 2720-2739. https://doi.org/10.1007/s10765-015-1977-1

Keyvani, M., Afrand, M., Toghraie, D., & Reiszadeh, M. (2018). An experimental study on the thermal conductivity of cerium oxide/ethylene glycol nanofluid: Developing a new correlation. *Journal of Molecular Liquids*, *266*, 211-217. https://doi.org/10.1016/j.molliq.2018.06.010

Khodadadi, H., Toghraie, D., & Karimipour, A. (2019). Effects of nanoparticles to present a statistical model for the viscosity of MgO-Water nanofluid. *Powder Technology*, *342*, 166-180. https://doi.org/10.1016/j.powtec.2018.09.076

Liou, T. M., Wei, T. C., & Wang, C. S. (2019). Investigation of nanofluids on heat transfer enhancement in a louvered microchannel with lattice Boltzmann method. *Journal of Thermal Analysis and Calorimetry*, *135*(1), 751-762. https://doi.org/10.1007/s10973-018-7299-3

Noreen, S., Qasim, M., & Khan, Z. H. (2015). MHD pressure driven flow of nanofluid in curved channel. *Journal of Magnetism and Magnetic Materials*, *393*, 490-497. https://doi.org/10.1016/j.jmmm.2015.05.038

Pak, B. C., & Cho, Y. I. (1998). Hydrodynamic and heat transfer study of dispersed fluids with submicron metallic oxide particles. *Experimental Heat Transfer an International Journal*, *11*(2), 151-170. https://doi.org/10.1080/08916159808946559

Pakdaman, M. F., Akhavan-Behabadi, M. A., & Razi, P. (2012). An experimental investigation on thermo-physical properties and overall performance of MWCNT/heat transfer oil nanofluid flow inside vertical helically coiled tubes. *Experimental Thermal and Fluid Science*, *40*, 103-111. https://doi.org/10.1016/j.expthermflusci.2012.02.005

Rosensweig, R. E. (2013). *Ferrohydrodynamics*. Courier Corporation. Retrieved from https://books.google.mw/books?id=ng_DAgAAQBAJ&printsec=frontcover#v=onepage&q&f=false

Shabi, O. A., Alhazmy, M., Negeed, E. S. R., & Elzoghaly, K. O. (2024). Experimental investigation of shell and helical coiled heat exchanger with Al_2O_3 nano-fluid with wide range of particle concentration. *Frontiers in Mechanical Engineering*, *10*, Article 1386254. https://doi.org/10.3389/fmech.2024.1386254

Varkaneh, A. S., Nooshabadı, G. A. S., & Arani, A. A. A. (2023). Flow field and heat transfer of ferromagnetic nanofluid in presence of magnetic field inside a corrugated tube. *Journal of Thermal Engineering*, *9*(6), 1667-1686. https://doi.org/10.18186/thermal.1401685

Wu, Z., Wang, L., & Sundén, B. (2013). Pressure drop and convective heat transfer of water and nanofluids in a double-pipe helical heat exchanger. *Applied Thermal Engineering*, *60*(1-2), 266-274. https://doi.org/10.1016/j.applthermaleng.2013.06.051

Xin, R. C., & Ebadian, M. A. (1997). The effects of Prandtl numbers on local and average convective heat transfer characteristics in helical pipes. *Journal of Heat Transfer*, *119*(3), 467–473. https://doi.org/10.1115/1.2824120

Xuan, Y., & Roetzel, W. (2000). Conceptions for heat transfer correlation of nanofluids. *International Journal of Heat and Mass Transfer*, *43*(19), 3701-3707. https://doi.org/10.1016/S0017-9310(99)00369-5

Yarahmadi, M., Goudarzi, H. M., & Shafii, M. B. (2015). Experimental investigation into laminar forced convective heat transfer of ferrofluids under constant and oscillating magnetic field with different magnetic field arrangements and oscillation modes. *Experimental Thermal and Fluid Science*, *68*, 601-611. https://doi.org/10.1016/j.expthermflusci.2015.07.002